East European Journal of Physics. 4. 200–207 (2024)
DOI: 10.26565/2312-4334-2024-4-19 ISSN 2312-4334

STUDY OF THE COULOMB NUCLEAR INTERFERENCE OF ^{23}Al BREAKUP REACTION WITH DIFFERENT TARGETS

Surender*, **Ravinder Kumar**
Deenbandhu Chhotu Ram University of Science and Technology, Murthal(Sonipat), 131039, Haryana, India
*Corresponding Author e-mail: surender.schphy@dcrustm.org
Received September 1, 2024; revised October 19, 2024; in final form October 31, 2024; accepted November 6, 2024

The impact of Coulomb-diffraction interference on the one-proton removal breakup cross-section and the width of the longitudinal momentum distribution (LMD) has been investigated for the breakup reaction of the ^{23}Al nucleus with different light to the heavy target for energy 40-100MeV/nucleon. Sensitivity to the target size and incident energy was analyzed through calculations that incorporate Coulomb interactions to all orders, including the full multipole expansion and nuclear diffraction using the eikonal approximation in the Glouber model. The results indicate that both constructive and destructive interferences significantly impact the observables, with the effects being more pronounced for medium-mass targets than light or heavy targets.

Keywords: *Coulomb nuclear interference; Proton halo; LMD; Proton breakup; One proton-removal cross-section*

PACS: 25.60.Gc

1. INTRODUCTION

After the discovery of halo nuclei in 1985 [1,2], extensive experimental and theoretical research has been conducted to explore their unique nuclear structures and their significant role in nucleosynthesis reactions [3–15]. Advancements in accelerator facilities have greatly accelerated this field of research, leading to the discovery of numerous exotic nuclei near the neutron or proton drip lines. Breakup reactions have been one of the most frequently used methods to investigate these nuclei [16–20]. While the breakup mechanisms of loosely bound neutron-rich nuclei are well understood, those of loosely bound proton-rich nuclei present a more complex situation. In such cases, both the core of the projectile and the valence proton experience Coulomb interactions with the target, complicating the analysis, particularly when studying the Coulomb breakup mechanism exclusively [15, 16, 21]. Recent theoretical studies have demonstrated that this complexity affects observables such as breakup cross sections, the width of longitudinal momentum distributions, and angular distributions. Additionally, interference between diffraction and Coulomb breakup mechanisms has been reported to significantly influence these observables, depending on the size of the participating nuclei and the incident energies [22–27].

The study of single proton breakup from proton-rich nuclei via the Coulomb breakup mechanism is directly linked to astrophysical proton capture reactions through the detailed balance theorem [28, 29]. Precise values of Coulomb breakup observables are crucial inputs for estimating the reaction rates of proton capture reactions [13, 15, 30]. Therefore, it is essential to gain a deeper understanding of the Coulomb breakup mechanism and its interference with nuclear diffraction mechanisms to accurately derive astrophysical information.

In this study, we investigate the interference between Coulomb and diffraction mechanisms in the breakup of ^{23}Al at beam energies of 60 and 100 MeV/nucleon for various target cases, extending our previous work [31] to explore the trend of interference effects across a beam energy range of 40-100 MeV/nucleon. We analyze the impact of interference on single proton breakup cross-sections and the full width at half maximum (FWHM) of core longitudinal momentum distributions (LMD) for different targets and examine the sensitivity of these observables to the incident energies. The calculations account for Coulomb interactions to all orders, including full multipole expansion, and treat nuclear diffraction within the eikonal approximation [23, 27]. The calculations are performed in the absence and presence of each mechanism, allowing us to clearly identify the role of interference between the breakup mechanisms.

The ^{23}Al nucleus is chosen for this investigation because it is a proton-rich nucleus located near the proton drip line, with a very low proton separation energy of S_p = 141.11(43) keV [15], and its significant astrophysical implications as noted in [21, 32, 33]. In a recent experimental study [15], the measurement of core fragment momentum distribution and breakup cross-section was used to extract spectroscopic factors and asymptotic normalization coefficients (ANCs) [32, 34–36], which were subsequently employed to determine the stellar reaction rate for the direct radiative proton capture reaction $^{22}Mg(p,\gamma)^{23}Al$ [15].

Given the important role of ^{23}Al in the $^{22}Mg(p,\gamma)^{23}Al$ direct capture reaction, it is intriguing to investigate the interference between Coulomb and nuclear diffraction breakup mechanisms in the ^{23}Al breakup reaction, as these interferences may either enhance or suppress the single proton breakup cross-section and the LMD width, as reported in [26, 27]. This study has been conducted in light of previous works [26, 27]. The effect of uncertainty in the one-proton

Cite as: Surender, R. Kumar, East Eur. J. Phys. 4, 200 (2024), https://doi.org/10.26565/2312-4334-2024-4-19

separation energy (S_p = 141.11(43) keV) on breakup observables was found to be less than 5% for both light [37] and heavy targets.

2. THEORETICAL FORMALISM

We followed the theoretical formalism of ref. [23, 27], where the Coulomb potential between projectile and target is taken as

$$V(\vec{r},\vec{R}) = \frac{V_c}{\mid \vec{R}-\beta_1\vec{r} \mid} + \frac{V_v}{\mid \vec{R}+\beta_2\vec{r} \mid} - \frac{V_0}{\vec{R}} \tag{1}$$

where $V_c = Z_c Z_t e^2, V_v = Z_v Z_t e^2$, and $V_0 = (Z_v + Z_c)\, Z_t e^2$. β_1 and β_2 are the mass ratios of proton and core, respectively, to that of projectile. Z_c, Z_t and Z_v are the core, target and valence proton charges, respectively. Also $\vec{r}$ and $\vec{R}$ are the position vectors of core to proton and target to projectile, fig. 1 in ref. [26]. So the perturbed Coulomb phase for the whole projectile (core plus valence proton) is

$$\chi^p = \frac{2}{\hbar v}\left(V_c e^{i\beta_1\omega z/v} K_0\left(\omega b_c/v\right) - V_0 K_0\left(\omega R_\perp/v\right) + V_v e^{-i\beta_2\omega z/v} K_0\left(\omega b_v/v\right)\right), \tag{2}$$

where $\omega = \left(\varepsilon_f - \varepsilon_0\right)/\hbar$ and ε_0 is the valence nucleon binding energy while ε_f is the final nucleon-core continuum energy. The Coulomb potential for the entire projectile (V_0) can be expressed as the sum of the core (V_c) and valence proton (V_v) Coulomb potentials with respect to the target, i.e., $V_0 = V_c + V_v$. Consequently, the perturbed Coulomb phase for the entire projectile can be written as:

$$\chi^p = \chi\left(\beta_1, V_c\right) + \chi\left(-\beta_2, V_v\right) \tag{3}$$

where

$$\chi(\beta_1, V_c) = \frac{2V_c}{\hbar v}\left(e^{i\beta_1\omega z/v} K_0(\omega b_c/v) - K_0\left(\omega R_\perp/v\right)\right) \tag{4}$$

$$\chi(-\beta_2, V_v) = \frac{2V_v}{\hbar v}\left(e^{-i\beta_2\omega z/v} K_0(\omega b_v/v) - K_0\left(\omega R_\perp/v\right)\right) \tag{5}$$

corresponds to core- target Coulomb phase and valence proton-target Coulomb phase respectively. As series of work have stressed the importance of inclusion of Coulomb mechanism to all orders specially in proton halo breakup reactions [22–27]. Therefore, we have also treated the Coulomb interaction to all orders in sudden formalism for both core-target (called recoil interaction) and valence proton-target (called direct interactions), as discussed in detail in ref. [22–25], and respective Coulomb phases can be written as

$$g^{rec}(b_c) = \int d\vec{r} e^{-i\vec{k}\cdot\vec{r}}\phi_i(\vec{r})\left(e^{i\frac{2V_c}{\hbar v}\log\frac{b_c}{R_\perp}} - 1 - i\frac{2V_c}{\hbar v}\log\frac{b_c}{R_\perp} + i\chi(\beta_1, V_c)\right) \tag{6}$$

$$g^{dir}(b_v) = \int d\vec{r} e^{-i\vec{k}\cdot\vec{r}}\phi_i(\vec{r})\left(e^{i\frac{2V_v}{\hbar v}\log\frac{b_v}{R_\perp}} - 1 - i\frac{2V_v}{\hbar v}\log\frac{b_v}{R_\perp} + i\chi(-\beta_2, V_v)\right) \tag{7}$$

and nuclear diffraction dissociation amplitude is calculated in eikonal approximation as

$$g^{diff} = \int d\vec{r} e^{-i\vec{k}\cdot\vec{r}}\phi_i(\vec{r})\left(e^{i\chi_{nt}(b_v)} - 1\right) \tag{8}$$

So the core fragment momentum distribution can be written as

$$\frac{d\sigma}{d\vec{k}} = \frac{1}{8\pi^3}\int d\vec{b}_c |S_{ct}(b_c)|^2 |g^{rec} + g^{dir} + g^{diff}|^2 \tag{9}$$

and breakup cross section may be obtained by integrating the core fragment momentum distribution over the transverse component of momentum. Here, $S_{\rm ct}(b_c)$ and $e^{i\chi_{nt}(b_v)}$ represent the core-target and proton-target S matrices, which are calculated using the $t\rho\rho$ formalism through the standard MOMDIS code [38]. We employed Hartree-Fock nuclear density forms [39] for both the core and the targets. The projectile wave function, $\phi_i(\vec{r})$, was computed by numerically solving the Schrödinger equation for the Woods-Saxon nuclear potential with fixed geometry parameters: radius (r_0 = 1.25 fm), diffuseness (a_0 = 0.7 fm) [15], and spin-orbit coupling potential V_{ls} = −20.72 MeV [40], for the $[0^+ \otimes 1d_{5/2}]$ bound state configuration. The depth of the nuclear potentials was adjusted to reproduce the binding energy of the valence proton, S_p = 0.141 MeV.

The sensitivity of the breakup cross-section and longitudinal momentum distribution (LMD) width to the Woods-Saxon potential parameters (r_0 and a_0) was also evaluated for the 40 MeV/nucleon case. We found that the cross-section increased by approximately 20% as r_0 changed from 1.15 fm to 1.3 fm, while the FWHM of the LMD increased by less than 2-3%. Similarly, an increase in the cross-section of less than 10% was observed when a_0 was varied from 0.6 fm to 0.7 fm, with the LMD width increasing by less than 2-3%. This sensitivity is consistent with the results reported in [41]. Additional theoretical details of the formalism can be found in [22–25].

3. RESULTS AND DISCUSSION

The single proton breakup cross-section and core fragment momentum distribution were calculated for the ^{23}Al nucleus with ^{12}C, ^{58}Ni, and ^{208}Pb targets, in the beam energy range of 40-100 MeV/nucleon. The ^{23}Al nucleus is treated as a two-body system, consisting of a $[0^+ \otimes 1d_{5/2}]$ core plus a proton in a bound state configuration, resulting in $J^\pi = 5/2^+$. In this analysis, only the $1d_{5/2}$ state of the valence proton is considered, as predicted by the shell model and widely reported in the literature [15].

For the present calculations, we focused on 60 and 100 MeV/nucleon beam energies, as the 40 and 80 MeV/nucleon data had already been published in our previous work [31], though the table includes all energies from 40-100 MeV/nucleon. The objective was to examine how the breakup cross-section and FWHM of the parallel momentum distribution change with different beam energies and targets. The calculations were performed separately for nuclear diffraction breakup and Coulomb breakup mechanisms, as well as for the combined effect of both mechanisms, to observe the interference effects.

Table 1. Calculated one-proton removal breakup cross-section and FWHM of LMD for ^{12}C target at different incident beam energies corresponding to nuclear diffraction, pure Coulomb, nuclear diffraction with Coulomb mechanisms and percentage change in observables values

Beam energy(MeV/nucleon)	40		60		80		100	
	σ_{-p} (mb)	FWHM (MeV/c)	σ_{-p} (mb)	FWHM (MeV/c)	σ_{-p} (mb)	FWHM (MeV/c)	σ_{-p} (mb)	FWHM (MeV/c)
Diff.	10.37	164.24	16.45	178.30	13.65	177.59	9.46	178.50
Coul.(total)	5.27	121.33	4.30	128.76	3.92	135.40	3.50	139.14
Coul+Diff.(simple sum)	15.64	145.64	20.75	163.07	17.57	164.65	12.96	164.71
Coul+Diff.(Cal. together)	16.42	144.54	20.01	160.64	16.20	162.20	11.59	161.97
% change	+4.99	-0.75	-3.57	-1.49	-7.80	-1.48	-10.57	-1.66

Table 2. Calculated one-proton removal breakup cross-section and FWHM of LMD for ^{58}Ni target at different incident beam energies corresponding to nuclear diffraction, pure Coulomb, nuclear diffraction with Coulomb mechanisms and percentage change in observables values

Beam energy (MeV/nucleon)	40		60		80		100	
	σ_{-p} (mb)	FWHM (MeV/c)	σ_{-p} (mb)	FWHM (MeV/c)	σ_{-p} (mb)	FWHM (MeV/c)	σ_{-p} (mb)	FWHM (MeV/c)
Diff.	14.96	156.54	20.04	168.59	22.55	167.08	15.77	162.57
Coul.(total)	115.09	114.16	81.25	116.98	66.92	120.44	57.85	123.13
Coul+Diff. (simple sum)	130.05	117.83	103.81	124.20	86.96	127.72	73.62	129.31
Coul+Diff. (Cal. together)	156.90	125.43	127.49	130.24	105.04	132.23	87.82	132.75
% change	+20.65	+6.44	+22.81	+4.86	+20.79	+3.53	+19.28	+0.79

Calculated one-proton removal breakup cross-section and FWHM widths of the longitudinal momentum distribution (LMD) are presented in Tables 1-3. These results are shown exclusively for nuclear diffraction ($diff$), total Coulomb (recoil + direct) ($Coul$), the simple algebraic sum of total Coulomb and diffraction ($Coul + diff$ (simple sum)), and the total Coulomb and diffraction mechanisms calculated together ($Coul + diff$ (calculated together)). The rows correspond to the ^{12}C, ^{58}Ni, and ^{208}Pb targets for Tables 1, 2, and 3, respectively. The respective LMD results are illustrated in Figures 1-3, where the percentage change is calculated using the formula:

$$\frac{X^{(Coul+diff)} - (X^{Coul} + X^{diff})}{(X^{Coul} + X^{diff})} \times 100\%,$$

where X represents either the cross-section or the FWHM of the LMD. For simplicity, the spectroscopic factor is taken as unity throughout the calculations.

Table 1 shows the results for the ^{12}C target at 40, 60, 80, and 100 MeV/nucleon beam energies. At 40 MeV/nucleon, the Coulomb and diffraction mechanisms (calculated together) result in a cross-section increase of +5% compared to their simple sum, indicating constructive interference between the Coulomb and diffraction breakup mechanisms. However, at higher beam energies (60, 80, and 100 MeV/nucleon), destructive interference occurs, reducing the cross-section by -3.5% to -10.5%, with the magnitude of the reduction increasing as the beam energy increases. The interference effect on the FWHM of the LMD shows a slight destructive trend for all incident energies, reducing the width by -0.7% to -1.66%, with this variation mildly depending on the beam energy. In contrast, for the ^{12}C target, except at 40 MeV/nucleon (Fig. 1(a)),

the black solid curve appears lower than the green dash-dotted curve, indicating destructive interference, which reduces the cross-section. However, at 40 MeV/nucleon, the interference is constructive.

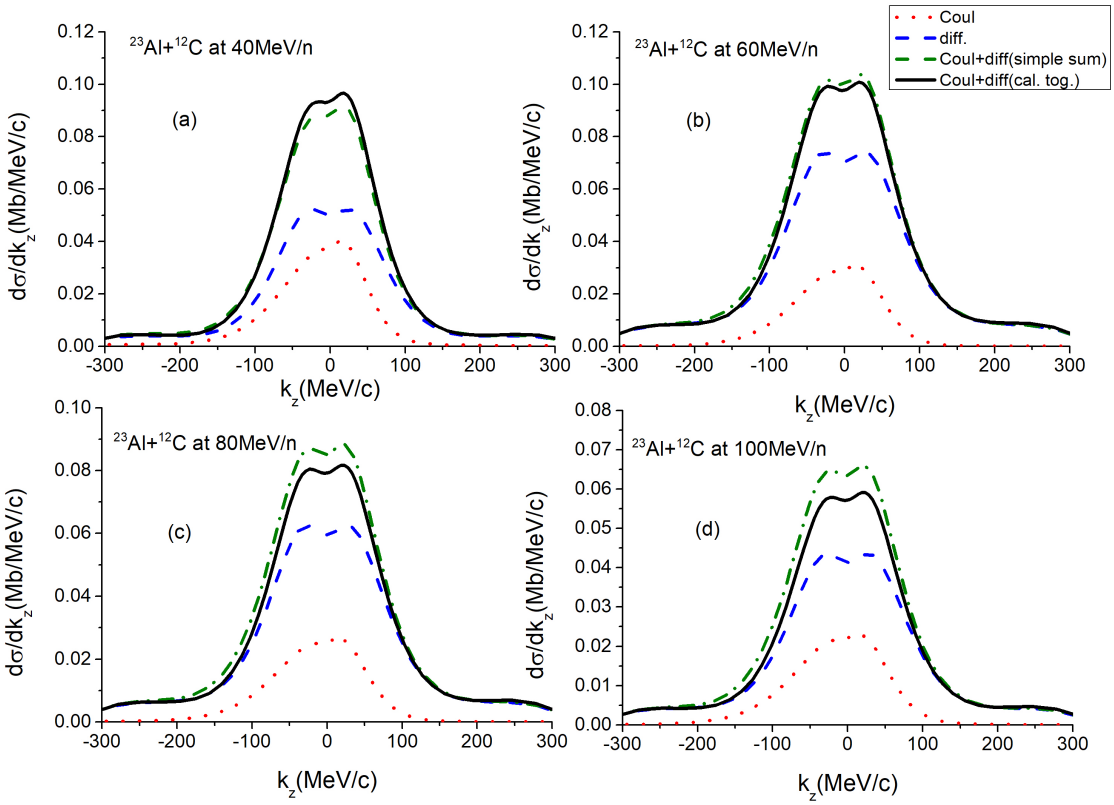

Figure 1. (Color online) Longitudinal Momentum Distribution for ^{12}C(^{23}Al, ^{22}Mg)X at 40-100 MeV/nucleon beam energies.

Table 3. Calculated one-proton removal breakup cross-section and FWHM of LMD for ^{208}Pb target at different incident beam energies corresponding to nuclear diffraction, pure Coulomb, nuclear diffraction with Coulomb mechanisms and percentage change in observables values

Beam energy (MeV/nucleon)	40		60		80		100	
	σ_{-p} (mb)	FWHM (MeV/c)	σ_{-p} (mb)	FWHM (MeV/c)	σ_{-p} (mb)	FWHM (MeV/c)	σ_{-p} (mb)	FWHM (MeV/c)
Diff.	21.45	153.73	32.32	166.13	29.26	163.91	21.94	157.98
Coul.(total)	2029.37	146.23	1162.78	134.62	821.72	129.78	638.78	127.64
Coul+Diff. (simple sum)	2050.81	146.34	1195.11	135.44	850.98	130.80	660.72	128.52
Coul+Diff. (Cal. together)	2077.99	152.13	1277.35	142.65	927.91	138.19	725.65	135.23
% change	+1.32	+3.96	+6.88	+5.32	+9.04	+5.65	+9.82	+5.22

For the ^{58}Ni target (Table 2), constructive interference is consistently observed across all incident energies, resulting in an enhancement of the breakup cross-section by approximately +20%. Additionally, the FWHM of the LMD increases from +6.4% to +0.79% as the incident energy increases, in comparison to the algebraic sum of the Coulomb and diffraction components calculated independently.

In the case of the ^{208}Pb target, as shown in Table 3, the breakup cross-section exhibits an increase ranging from +1.3% to +9.8% with increasing incident energy, while the FWHM of the LMD broadens by +3.96% to +5.22%. This behavior again indicates the presence of constructive interference between the Coulomb and nuclear breakup mechanisms.

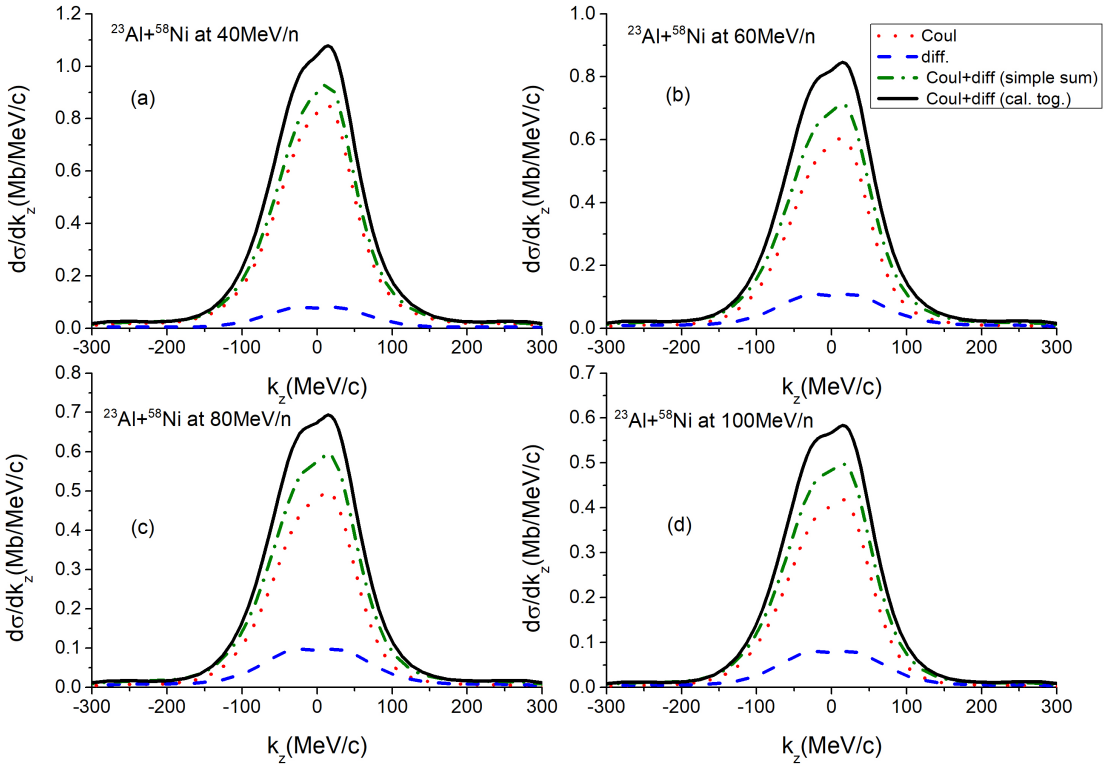

Figure 2. (Color online) Longitudinal Momentum Distribution for ^{58}Ni(^{23}Al, ^{22}Mg)X at 40-100 MeV/nucleon beam energies.

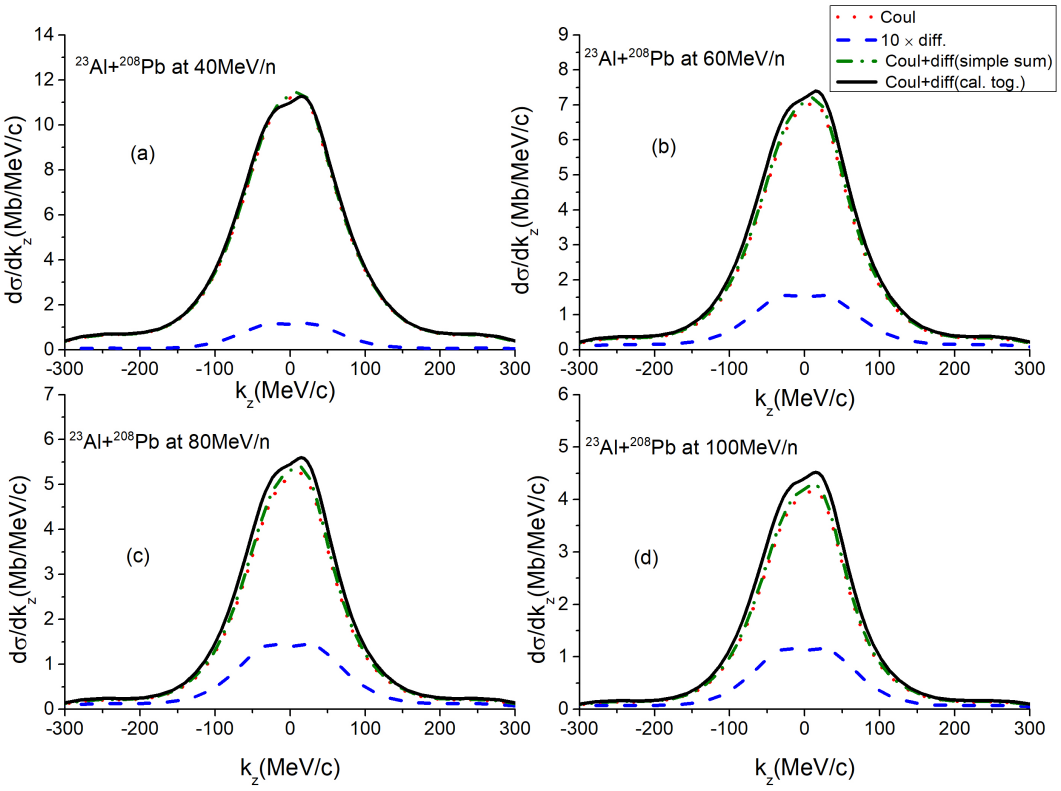

Figure 3. (Color online) Longitudinal Momentum Distribution for ^{208}Pb(^{23}Al, ^{22}Mg)X at 40-100 MeV/nucleon beam energies.

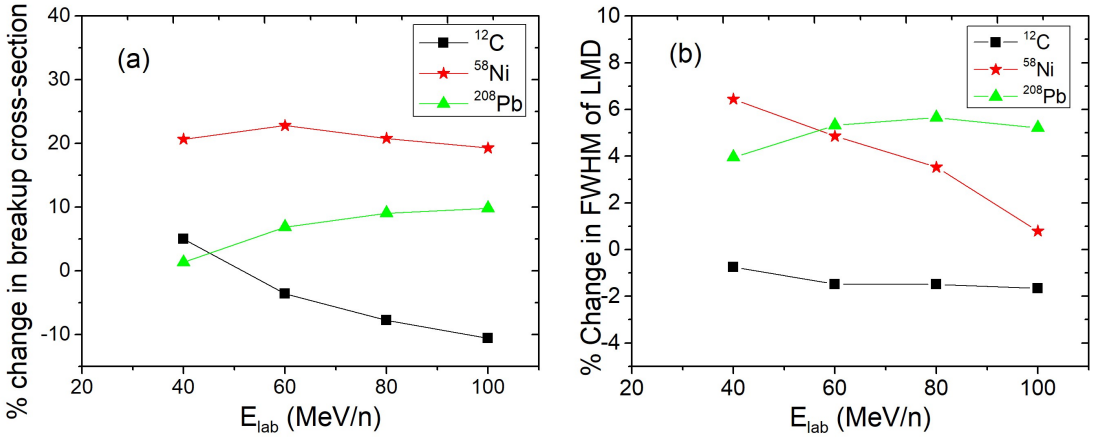

Figure 4. (Color online) (a) Variation of Percentage change in single proton breakup cross-section due to Coulomb diffraction interference with incident energy, (b) Variation of Percentage change in FWHM of LMD due to Coulomb diffraction interference with incident energy, in case of different target.

For enhanced clarity, Figures 1-3 present the LMD results for all target cases, where the diffraction component is represented by a blue dashed curve, the Coulomb component by a red dotted curve, their simple algebraic sum by a green dash-dotted curve, and the combined Coulomb and diffraction calculation by a black solid curve. For the ^{58}Ni and ^{208}Pb targets, the black solid curve (representing Coulomb and diffraction calculated together) consistently exceeds the green dash-dotted curve (representing the algebraic sum), thereby reflecting the constructive interference between the two breakup mechanisms, which leads to an enhancement in both the breakup cross-section and the LMD width. In our previous paper [31], we investigated the interference effects between recoil and direct breakup reactions, which were consistently found to be destructive for all target and beam energies. Therefore, in this paper, we do not provide the LMD or cross-sections; instead, the Coulomb calculations presented here reflect the result of the interference effect between recoil and direct breakup.

Figures 4(a) and 4(b) further illustrate the percentage variations in the single-proton breakup cross-section and the FWHM of the LMD as a function of incident energy for all targets. It is evident from these figures that the trend of percentage variations differs between targets, exhibiting behavior consistent with the results reported in Ref. [24]. Thus, we observed that for medium-mass targets such as ^{58}Ni, the magnitude of constructive interference is greater compared to ^{12}C and ^{208}Pb. This can be attributed to the fact that, for smaller targets, the dominant reaction mechanism causing the breakup is nuclear interaction, with Coulomb interaction being relatively insignificant. In contrast, for heavier targets, the Coulomb interaction tends to dominate over the nuclear interaction, driving the breakup process. For medium-mass targets, both Coulomb and nuclear interactions play significant roles during the interaction between the projectile and target, making the interference between Coulomb and nuclear mechanisms more pronounced and significantly affecting the breakup observables. This observation suggests that when designing experiments with proton-rich nuclei, it may be beneficial to choose either light or heavy targets to minimize the impact of interference on the breakup observables. However, further detailed investigation is needed to fully understand the complex interference mechanisms in breakup reactions.

4. CONCLUSIONS

The investigation examines the Coulomb-diffraction interference present during the single-proton breakup reaction of the ^{23}Al nucleus. The study analyzes the interference effects on the single-proton breakup cross-section and the full-width at half maximum (FWHM) of the longitudinal momentum distribution (LMD) of core fragments for targets ^{12}C, ^{58}Ni, and ^{208}Pb. Sensitivity to target size and incident energy was systematically assessed by performing calculations at commonly used incident beam energies - 40, 60, 80, and 100 MeV/nucleon for each target.

The results indicate that Coulomb-diffraction interference can be either constructive or destructive, leading to significant variations in the observable values. The magnitude of these variations is sensitive to both target size and incident energy, with the effect being most enhancement in breakup cross-section for medium-mass targets compared to light or heavy targets. This finding highlight the need for careful consideration when dealing with reactions involving medium-mass targets. For greater clarity, we will further explore our breakup formalism in the upcoming studies by examining the angular distribution. This study represents a step towards a quantitative understanding of Coulomb-diffraction interference in ^{23}Al breakup reactions. It aims to aid in the planning of future breakup experiments, helping to either minimize or avoid interference effects to obtain clearer and more accurate information.

Data Availability Statement: This manuscript has no associated data or the data will not be deposited.

ORCID

Surender, https://orcid.org/0000-0002-5306-3115; **Ravinder Kumar**, https://orcid.org/0000-0002-4992-2394

REFERENCES

[1] I. Tanihata, et al., Phys. Rev. Lett. **55**, 2676 (1985). https://doi.org/10.1103/PhysRevLett.55.2676

[2] I. Tanihata, et al., Physics Letters B, **160**(6), 380, (1985). https://doi.org/10.1016/0370-2693(85)90005-X

[3] T. Nakamura, et al., Physical Review C, **79**(3), 035805 (2009). https://doi.org/10.1103/PhysRevC.79.035805

[4] G. Baur, et al., Progress in Particle and Nuclear Physics, **51**(2), 487 (2003). http://dx.doi.org/10.1016/S0146-6410(03)90006-8

[5] G. Baur, et al., Progress in particle and nuclear physics, **59**(1), 122 (2007). https://doi.org/10.1016/j.ppnp.2006.12.002

[6] L.V. Grigorenko, et al., Physics Letters B, **641**(3-4), 254 (2006). https://doi.org/10.1016/j.physletb.2006.08.054

[7] C.A. Bertulani, et al., Physics Reports, **485**(6), 1959 (2010). https://doi.org/10.1016/j.physrep.2009.09.002

[8] L. Trache, et al., Physical review letters, **87**(27), 271102 (2001). https://doi.org/10.1103/PhysRevLett.87.271102

[9] L.Trache et al., Physical Review C, **66**(3), 035801 (2002). https://doi.org/10.1103/PhysRevC.66.035801

[10] V.E. Iacob, et al., Physical Review C, **74**(4), 045810 (2006). https://doi.org/10.1103/PhysRevC.74.045810

[11] S.S. Chandel, et al., Physical Review C, **68**(5), 054320 (2003). https://doi.org/10.1103/PhysRevC.68.054320

[12] M.M. Khansari, et al., New Astronomy, **57**, 76 (2017). https://doi.org/10.1016/j.newast.2017.06.013

[13] T.L. Belyaeva, et al., Physical Review C, **80**(6), 064617 (2009). https://doi.org/10.1103/PhysRevC.80.064617

[14] V.S. Melezhik, et al., Physical Review C, **64**(5), 054612 (2001). https://doi.org/10.1103/PhysRevC.64.054612

[15] A. Banu, et al., Physical Review C, **84**(1), 015803 (2011). https://doi.org/10.1103/PhysRevC.84.015803

[16] K. Hencken, et al., Physical Review C, **54**(6), 3043 (1996). https://doi.org/10.1103/PhysRevC.54.3043

[17] V.S. Melezhik, et al., Physical Review C, **59**(6), 3232 (1999). https://doi.org/10.1103/PhysRevC.59.3232

[18] N. Fukuda, et al., Physical Review C, **70**(5), 054606 (2004). https://doi.org/10.1103/PhysRevC.70.054606

[19] S. Typel, et al., Physical Review C, **64**(2), 024605 (2001). https://doi.org/10.1103/PhysRevC.64.024605

[20] R. Chatterjee, et al., Nuclear Physics A, **675**(3-4), 477 (2000). https://doi.org/10.1016/S0375-9474(00)00179-2

[21] T. Gomi, et al., Journal of Physics G: Nuclear and Particle Physics, **31**(10), S1517 (2005). https://doi.org/10.1088/0954-3899/31/10/023

[22] A. Garcia-Camacho, et al., Nuclear Physics A, **776**(3-4), 118 (2006). https://doi.org/10.1016/j.nuclphysa.2006.07.033

[23] A. García-Camacho, et al., Physical Review C, **76**(1), 014607 (2007). https://doi.org/10.1103/PhysRevC.76.014607

[24] J. Margueron, et al., Nuclear Physics A, **703**(1-2), 105 (2002). https://doi.org/10.1016/S0375-9474(01)01336-7

[25] J. Margueron, et al., Nuclear Physics A, **720**(3-4), 337 (2003). https://doi.org/10.1016/S0375-9474(03)01092-3

[26] R. Kumar, and A. Bonaccorso, Physical Review C, **84**(1), 014613 (2011). https://doi.org/10.1103/PhysRevC.84.014613

[27] R. Kumar, and A. Bonaccorso, Physical Review C, **86**(6), 061601 (2012). https://doi.org/10.1103/PhysRevC.86.061601

[28] G. Baur, et al., Nuclear Physics A, **458**(1), 188 (1986). https://doi.org/10.1016/0375-9474(86)90290-3

[29] H. Rebel, in: Nuclear Astrophysics: Proceedings of a Workshop,FRG, (Springer, 1987), pp. 38-53.

[30] F. Schümann, et al., Physical Review C - Nuclear Physics, **73**(1), 015806 (2006). https://doi.org/10.1103/PhysRevC.73.015806

[31] Surender, and R. Kumar, Acta Physica Polonica B, **54**(9), (2023). https://doi.org/10.5506/APhysPolB.54.9-A1

[32] X.Y. Li, et al., Chinese Physics C, **44**(7), 074001 (2020). https://doi.org/10.1088/1674-1137/44/7/074001

[33] R.N. Panda, et al., Physics of Atomic Nuclei, **81**(4), 417 (2018). https://doi.org/10.1134/S1063778818040154

[34] F. De-Qing, et al., Chinese Physics Letters, **22**(3), 572 (2005). https://doi.org/10.1088/0256-307X/22/3/015

[35] D.Q. Fang, et al., Physical Review C, **76**(3), 031601 (2007). https://doi.org/10.1103/PhysRevC.76.031601

[36] Y.-L. Zhao, et al., Chinese physics letters, **20**(1), 53 (2003). https://doi.org/10.1088/0256-307X/20/1/316

[37] Surender, and R. Kumar, DAE Symp. Nucl. Phys. **66**, 691 (2023). https://www.sympnp.org/proceedings/66/B174.pdf

[38] C.A. Bertulani, and A. Gade, Computer Physics Communications, **175**(5), 372 (2006). https://doi.org/10.1016/j.cpc.2006.04.006

[39] Experimental Nuclear Reaction Data. National nuclear data center. Brookhaven National Laboratory (http://www. nndc. bnl. gov/exfor/exfor00. htm) and International Atomic Energy Agency, Nuclear Data Services, (http://www-nds. iaea. org/exfor/exfor. htm), 2000.

[40] W. Horiuchi, et al., Physical Review C, **81**(2), 024606 (2010). https://doi.org/10.1103/PhysRevC.81.024606

[41] X.Y. Zhao, et al., Physical Review C, **100**(4), 044609 (2019). https://doi.org/10.1103/PhysRevC.100.044609

ДОСЛІДЖЕННЯ КУЛОНОВСЬКОЇ ЯДЕРНОЇ ІНТЕРФЕНЦІЇ РЕАКЦІЇ РОЗПАДУ ^{23}Al З РІЗНИМИ МІШЕНЯМИ

Сурендер, **Равіндер Кумар**

[a] *Департамент математики, Відья Бхарати Махавідьяля, Кемп, Амраваті, 444601, Індія*

Вплив інтерференції кулонівської дифракції на поперечний переріз розпаду відриву одного протона та ширину розподілу поздовжнього імпульсу (LMD) було досліджено для реакції розпаду ядра ^{23}Al з різним світлом від важка мішень на енергію 40-100 МеВ/нуклон. Чутливість до розміру мішені та енергії падіння аналізувалася за допомогою розрахунків, які включають кулонівські взаємодії для всіх порядків, включаючи повне мультипольне розширення та ядерну дифракцію з використанням наближення ейконала в моделі Глоубера. Результати показують, що як конструктивні, так і деструктивні перешкоди суттєво впливають на спостережувані, причому ефекти більш виражені для цілей середньої маси, ніж для легких або важких цілей.

Ключові слова: *кулонівська ядерна інтерференція; протонне гало; LMD; розпад протона; поперечний переріз видалення одного протона*